Preparation and Characterization of Antimony-doped Tin Dioxide Interlayer and β-PbO₂ Film on Porous Titanium

Longyao Wang, Fanrong Pan, Lan Wang

Jiangsu Key Laboratory of Advanced Catalytic Materials and Technology, Key Laboratory of Fine Chemicals Technology of Jiangsu Province, School of petrochemical engineering, Changzhou University, Changzhou 213164, China
*E-mail: wang.longyao@cczu.edu.cn

The interlayer of antimony-doped tin dioxide (ATO) and β-PbO₂ film were prepared on porous titanium by thermal decomposition method and electrodeposition technology, respectively. The characterization results suggest that ATO can combine with porous titanium closely and form a solid solution on the substrate surface. Different from the dense plate based ATO, the surface of porous titanium-based ATO layer is smooth and no "mud crack" phenomenon, which can keep titanium from oxidation. The crystal of β-PbO₂ produced by electrodeposition attached on the porous surface and formed a solid film. Furthermore, the porous titanium-based β-PbO₂ prepared in this work shows porous structure. The average pore size of the novel composite material is 3.0 μm and the open porosity is 16.9%. The specific surface area of the material is $0.41 \text{ m}^2 \cdot \text{g}^{-1}$ which is nearly 10 times than that of porous titanium. According to the experiment results, the oxygen evolution potential of the porous titanium-based β-PbO₂ is 1.85 V and the calculated service life is more than 7 years.

1. INTRODUCTION

β-PbO₂ has excellent performances as good conductivity, high oxygen evolution potential and corrosion resistance, and it is used as anode material widely in the electrolysis processes for chemical production and water treatment [1, 2]. However, because β-PbO₂ is fragile and easy broken, it usually needs support in the processes of application [3, 4]. Titanium is one of the preferred supports with excellent mechanical strength. The thermal expansion ratios of titanium and β-PbO₂ are nearly the same, which can keep the β-PbO₂ layer and the support combining closely [5]. However, titanium is easily oxidized and form passive film on the interface of Ti/β–PbO₂. The passive film will increase the

resistance of the conductor and decrease the adhesion strength of Ti/β-PbO$_2$. In this case the β-PbO$_2$ layer will be peeled off quickly under the condition of gas erosion [6, 7]. Preparing a dense middle layer can protect titanium from oxidization. However, the middle layer often shows complex cracks when prepared on the plate surface of Ti, which degreased the performance of the electrode [8].

Porous titanium has the advantages as big specific surface and porous structure [9]. The non-planar structure provides sufficient stress compensating for the adhesion layer, which can reduce or avoid the cracks appearing in the layer. Moreover, the porous material can provide more active area for electrode, at the same time provide the convenient channels for the mass transfer between the active surfaces. Different with the dense based β-PbO$_2$ [10, 11], β-PbO$_2$ is prepared based porous titanium with the interlayer of Antimony doped Tin Oxide (ATO) in this paper.

2. MATERIALS AND METHOD

The porous titanium-based ATO interlayer and the β-PbO$_2$ film are prepared as follows: (1). Pretreatment. Cutting porous titanium (thickness 1mm, pore porosity 21.6%, average pore diameter 2.76 μm) to desired size; ultrasonic cleaning 5 min in acetone and then washing clear by deionized water; immersing in H$_2$SO$_4$ solution (20%wt, 80 ℃) 30 min and then washing clear by deionized water; Dried and prepared for next step. (2). Coating ATO. Loading the solution (SnCl$_4$·5H$_2$O 2.63mol/L, SbCl$_3$ 0.07mol/L, N-Butanol 80%v/v, HCl 20%v/v) on the surface of titanium by dip-coating method and then drying at 150 ℃ (repeat 5 times); sintering in the air atmosphere at 450℃ for 15min, and then cooled for next step. (3). Electrodepositing β-PbO$_2$. Under the experiment conditions (25 ℃, copper cathode, the spacing between electrodes 1 cm), electrodepositing the anode (porous titanium coated ATO) for a certain time in the electroplating solution (Pb(NO$_3$)$_2$ 0.45 mol/L, Cu(NO$_3$)$_2$ 0.27 mol/L, NaF 0.01mol/L).

The morphology surface of the materials is detected by SEM (JSM-6360LA and SUPRA55). The specific surface area is measured by Rapid specific surface area analyzer (Autosorb-iQ2-MP). The pore size and distribution is measured by bubble-pressure method (ASTM F316) [12]. The porosity of overall-pore is calculated with volume-density method, and the porosity of open-pore is calculated with liquid immersion method [13]. The crystal structure on the surface of the porous material is characterized by XRD (D/max 2500 PC). The life of the electrode is examined by accelerated life test [14] under high current density (25 ℃, 1mol/L H$_2$SO$_4$, electrode area 1cm^2, copper cathode, spacing between electrodes 1cm, current density 4A/cm^2). The service life can be calculated by the following equation:

$$t_0 = \left(\frac{i_t}{i_0}\right)^2 \times \frac{t}{24 \times 365} \tag{1}$$

Where t_0 is the service life, year; t is the test life, h; i_t is the test current density, mA·cm^{-2}; i_0 is the applied current density in industry, mA·cm^{-2}.

3. RESULTS AND DISCUSSION

3.1. The pretreatment of porous titanium

The porous titanium was prepared in our previous work upon powder metallurgy technology [10]. Porous titanium is an excellent metal porous material with the advantages as low density and high specific strength [15, 16]. The morphology of porous titanium shows typical particle packing appearance (Fig. 1a). The surface of the particles is smooth, and the sintering necks connected the particles (Fig. 1b). However, titanium is corroded by H_2SO_4 in the process of pretreatment and the morphology of porous titanium is different. Many fine particles disappeared (Fig. 1c), and the surface of the particles is covered with honeycomb dent (Fig. 1d).
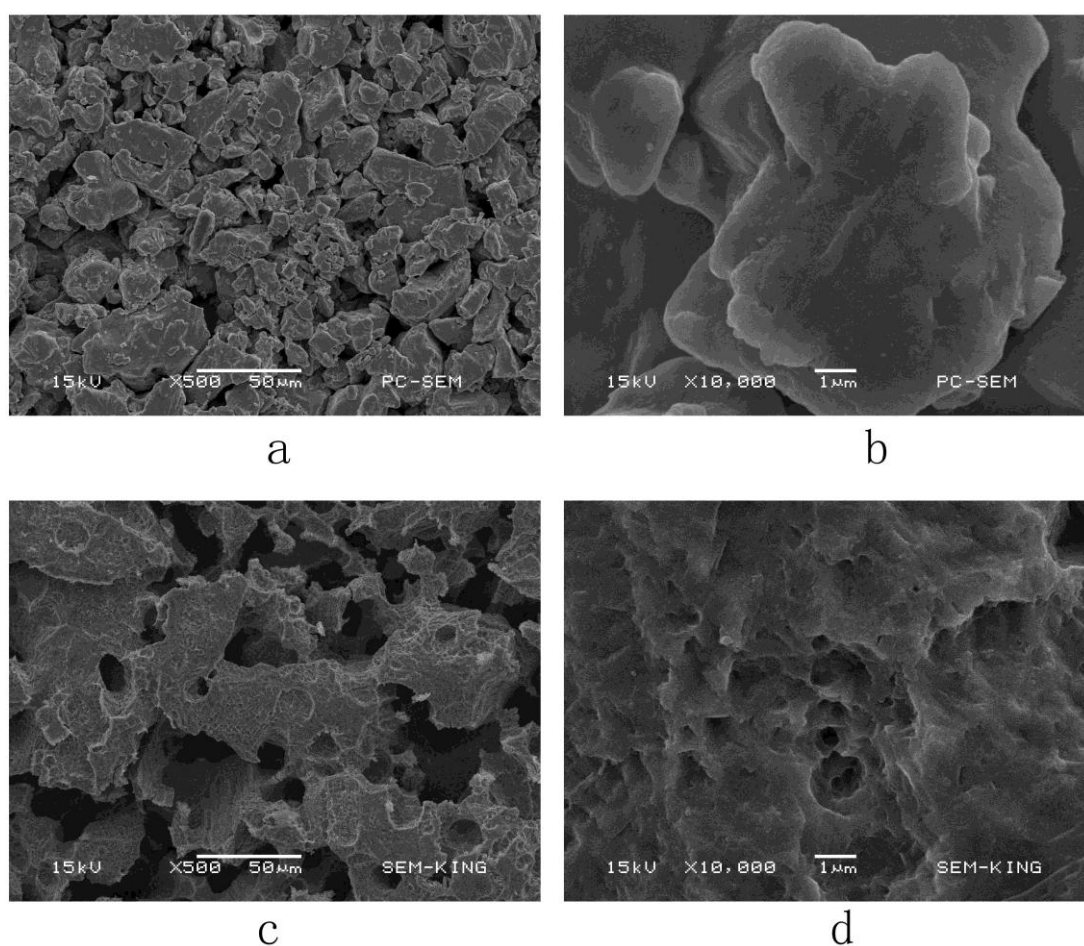

Figure 1. The morphology of porous titanium (a, b - before pretreatment; c, d - after pretreatment)

Fig. 2 shows the pore size distribution of porous titanium. It can be seen from Fig. 2 that the peak of the pore size distribution curve move forward after pretreatment, and a platform (3.5−5.5 μm) appeared on the new curve. The pore size of porous titanium increased and the average pore size increased from 2.6μm to 3.4μm after pretreatment, which coincide with the SEM images in Fig. 1.
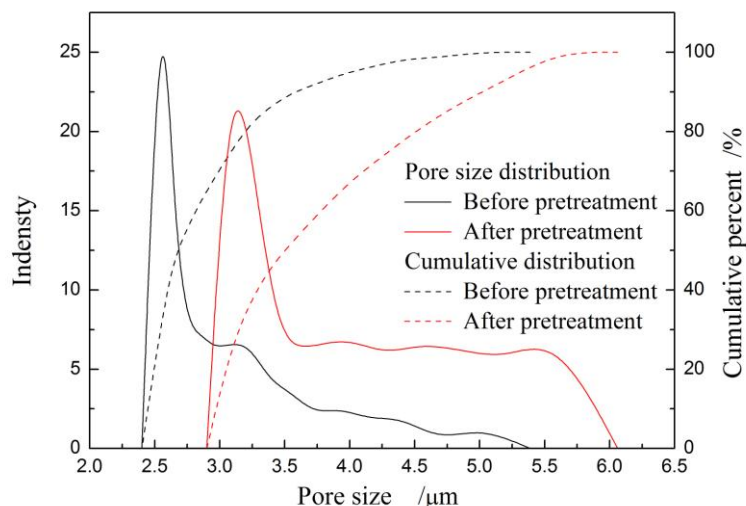
Figure 2. The pore size distribution of porous titanium

3.2. *The effects of substrate surface structure on ATO coating*

In the processes of electro-oxidation, the bare surface of titanium anode will be oxidized and form passive film (TiO_2) [17]. The resistivity of titanium (TA1) is $0.47 \times 10^{-6} \Omega \cdot m$ at 20 °C, while the resistivity of TiO_2 is $10^8 \Omega \cdot m$ approximately [18]. The passive film will degrade the performance and reduce the service life of the electrode.

SnO_2 is an n-type semiconductor. The resistivity of SnO_2 is about $5 \times 10^{-3} \Omega \cdot m$. Generally doping Sb^{5+} (6% mol/mol) in SnO_2 may reduce its resistivity significantly [19]. ATO shows good electrical conductivity and higher oxygen evolution potential. Because the lattice size of SnO_2 is closed to that of TiO_2, they can generate a dense solid solution, which may prevent TiO_2 film forming on the surface. Therefore, ATO can be used as the protective layer on the titanium surface.
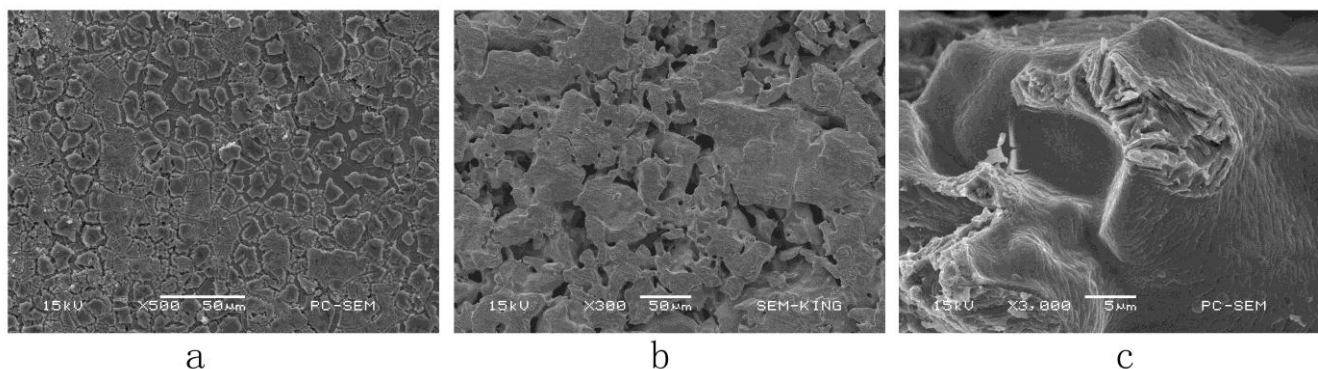

Figure 3. The morphology of titanium covered with ATO (a, surface of dense titanium; b, surface of porous titanium; c, cross section of porous titanium)

However, as showing in Fig. 3a, under the actions of internal stress, the ATO layer coated on the surface of dense titanium crack into pieces and appears "mud crack" phenomenon [20-22]. These cracks will degrade or disable the protective effects from ATO layer. Different from Fig. 3a, it can be seen from Fig. 3b that the ATO layer coated on the surface of porous titanium is undamaged. Although the surface is not smooth, but the obvious "mud crack" disappeared. The cross-section of porous titanium (Fig. 3c) also shows that ATO formed dense protective layer and combined with titanium tightly.

It can be speculated that the complex surface morphology of porous titanium (Fig. 1) provide effective stress compensating for the adhesion layer. Moreover, it should be noted that the particle size is growing when the sinter temperature is higher than 600 ℃ [23], then oxygen may penetrate into ATO layer and titanium will be oxidized.

3.3. The electrodeposition of β-PbO$_2$ film

In this work, β-PbO$_2$ film was electrodeposited on the surface of the support (porous titanium with ATO layer). It can be seen from Fig. 4 that the β-PbO$_2$ film deposited on the surface of the porous material uniformly. Although the average pore size decreased 20% (from 3.75 μm to 3.1 μm) after coating PbO$_2$, but the shape of the pores distribution curve almost the same.
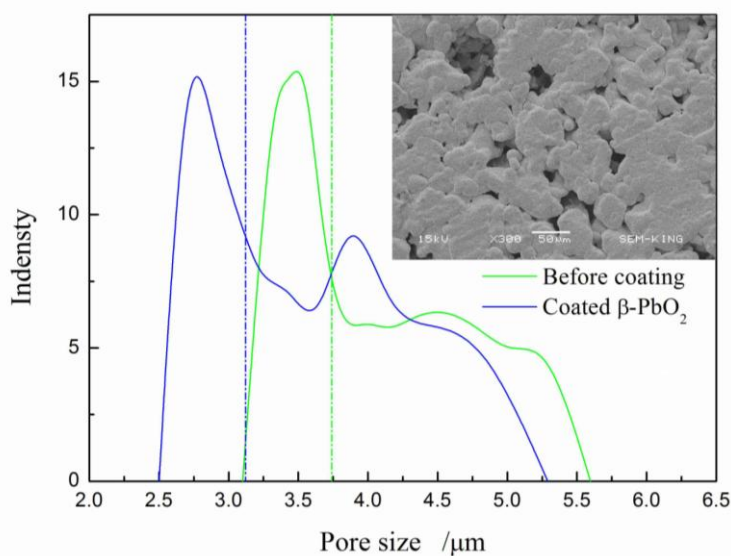

Figure 4. The pores distribution results and SEM image of porous titanium covered with β-PbO$_2$ (the vertical lines marked different average pore size)

The polymorphs of PbO$_2$ are known as orthorhombic α-PbO$_2$ and tetragonal β-PbO$_2$. The catalytic activity of β-PbO$_2$ is fairly high than that of α-PbO$_2$. Usually β-PbO$_2$ can be obtained by electrodeposition method under acid environment. The XRD result of the layer electrodeposited in this work is shown in Fig. 5. It can be seen from Fig. 5 that the result coincides with the standard XRD

spectrum of β-PbO$_2$. The SEM picture in Fig. 5 also shows that the size of the β-PbO$_2$ crystal is 1 μm approximately.
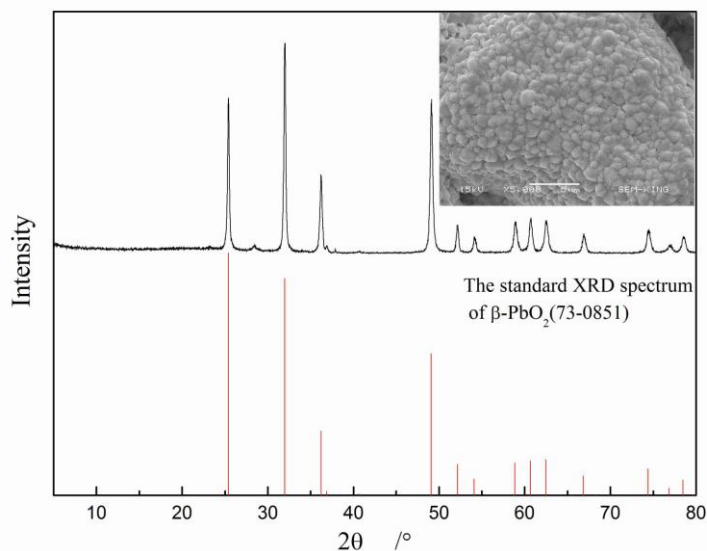

Figure 5. The XRD and SEM results of the β-PbO$_2$ layer

3.4. The effects of preparation process on porosity and specific surface area

Different from the traditional dense titanium-based β-PbO$_2$, the porous titanium-based β-PbO$_2$ has more specific surface area and high porosity. Tab. 1 shows the differences of porosity and specific surface area during the preparing processes, and Fig. 6 shows the differences of the pores distribution during the porous titanium-based β-PbO$_2$ preparing processes.

Table 1. The differences of porosity and specific surface area during the porous titanium-based β-PbO$_2$ preparing processes

Sample	Porosity /%	Open porosity /%	Closed porosity /%	Specific surface area /m$^2 \cdot$g^{-1}
Porous titanium	21.6	17.5	4.1	0.044
After pretreatment	26.2	24.2	2.1	0.49
After coating ATO*	24.1	22.1	2.0	0.16
After coating β-PbO$_2$ **	20.4	16.9	3.5	0.41

* Dip-coating and drying 5 times. ** Electrodeposition condition: 30 mA$\cdot$cm^{-2}, 25 °C, 20 min.

As can be seen from Tab. 1 and Fig. 6, the porosity of porous titanium increased 4.6% and the open porosity increased 6.7% after pretreatment. Because of the disappearance of the fine particles, the measure values of the maximum, minimum and average sizes of the pores are all increased. Especially the specific surface area is increased more than 10 times. However, due to the filling effect and the disappearance of tiny pore, the porosity and open porosity of porous titanium are decreased about 2% after coating ATO. The maximum size of the pores decreased, while the minimum size of the pores increased. The specific surface area decreased 0.33 $m^2 \cdot g^{-1}$ and the scope of pores distribution reduced 0.77 μm, but the average pore size nearly the same as before. After coating β-PbO$_2$, the measure values of porosity, open porosity and the pore size are all decreased. However, because of the crystal of the β-PbO$_2$ provided more surface area, although the average pore size reduced to 3.1 μm, the specific surface area increases to 0.41 $m^2 \cdot g^{-1}$.
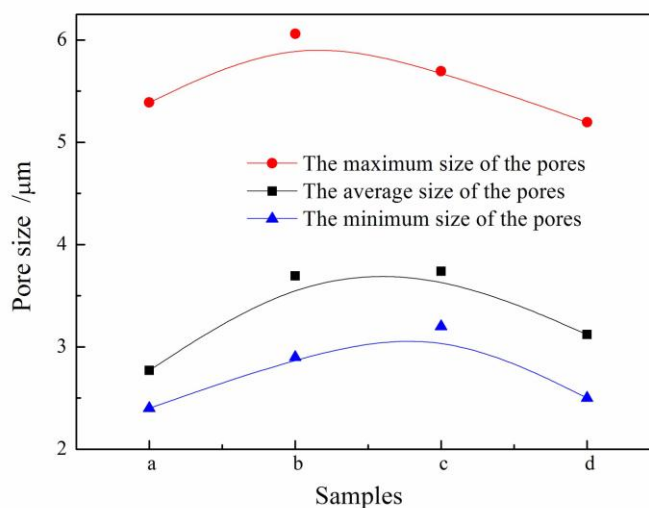

Figure 6. The changes of pore size during the porous material preparation processes (a, Porous titanium; b, After pretreatment; c, After coating ATO; d, After electrodepositing β-PbO$_2$)

3.5. The oxygen evolution potential and anode life of porous titanium-based β-PbO$_2$

The porous titanium-based β-PbO$_2$ can be used as anode in the processes of electrolysis. Among the anodic reactions, the side reaction is mainly oxygen evolution reaction. The higher oxygen evolution potential of the anode is helpful to degrade the adverse reactions and improve the current efficiency. The oxygen evolution potential of the porous titanium based β-PbO$_2$ electrode is measured in 0.5 mol·L^{-1} H$_2$SO$_4$ solution. The result in Fig.7 shows that the oxygen evolution potential is 1.85 V, which is close to the value 1.83V (Ti/CeO$_2$-F-PbO$_2$) reported before [24].

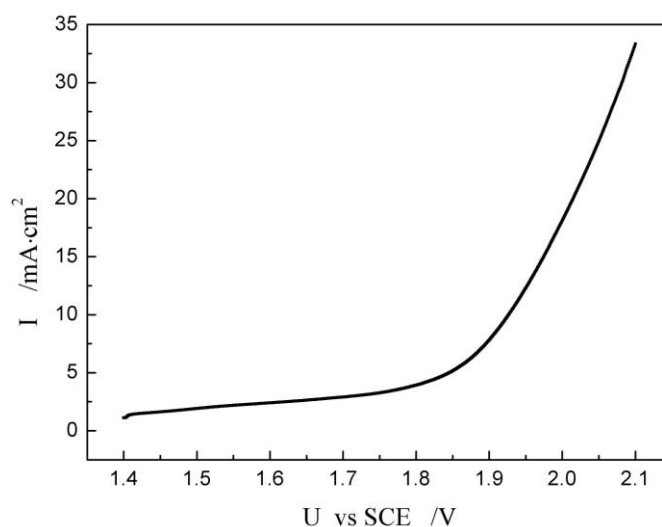**Figure 7.** Oxygen evolution potential curve of Ti/ATO/β–PbO$_2$ in 0.5 mol·L^{-1} H$_2$SO$_4$ solution

The surface passivation, the consumption of active layer and the surface contamination are all affected the service life of the electrode [25]. According to the results from the electrode accelerated life test and Eq.(1), the calculated service life of the prepared electrode is more than 7 years under the current density 50 mA·cm^{-2}.

4. CONCLUSION

A novel composite material with ATO interlayer and β-PbO$_2$ film was prepared on porous titanium by thermal decomposition method and electrodeposition technology, respectively. The characterization results suggest that ATO combined with titanium closely and formed a solid solution. The porous titanium provide effective stress compensating for the adhesion layer and the ATO layer on the surface of porous titanium is undamaged and without "mud crack" phenomena.

The size of β-PbO$_2$ crystal is 1 μm approximately and packed closely on the surface of the porous material. According to the experiment results of the porous titanium-based β-PbO$_2$, the specific surface area, the porosity and the average pore size are 0.41 m^2·g^{-1}, 20.4% and 3.0 μm respectively. The oxygen evolution potential of the porous titanium based β-PbO$_2$ electrode is 1.85 V in 0.5 mol·L^{-1} H$_2$SO$_4$ solution, and the calculated service life is more than 7 years under the current density 50 mA·cm^{-2}.

Reference

1. X. Ma, R. Wang, W. Guo, H. Yang and Z. Liang, *Int. J. Electrochem. Sci.*, 7 (2012) 6012.
2. Z.Q. He, C.X. Huang, Q. Wang, Z. Jiang, J. Chen and S. Song, *Int. J. Electrochem. Sci.*, 6 (2011) 4341.
3. X.Y. Duan, F. Ma and Z.X. Yuan, *Electroplating & Finishing*, 31 (2012) 5.
4. H.Y. Li, Y.H. Zhang, Y. Chen, W.Q. Han and L.J. Wang, *J. Adv. Mater. Res.*, 391 (2011) 1273.
5. H.S. Xun, H.B. Lin, and H.Y. Lu, *The 6th National Conference on Environmental Chemistry*. 2011.
6. H. An, Q. Li, D.J. Tao, H. Cui, X.T. Xu, L. Ding, L. Sun and J.P. Zhai, *Appl. Surf. Sci.*, 258 (2011) 218.
7. X.B. Ren, H.Y. Lu, Y.N. Liu, W. Li and H.B. Lin, *Acta. Chim. Sinica.*, 67 (2009) 888.
8. H. Xu, W. Yan and L. Chang, *Rare. Metal. Mat. Eng.*, 41 (2012) 462.
9. L.T. Guo, X.C. Liu, J.Q. Gao, J.F. Yang, T.W. Guo and Y.B. Zhu, *Mater. Manuf. Process.*, 25 (2010) 710.
10. L. Wang, P. Liu, L.Y. Wang, W.H. Xing, Y.Q. Fan and N.P. Xu, *Mater. Manuf. Process.*, 28 (2013) 1166.
11. H. You, Y.H. Cui, Y.J. Feng, J.F. Liu and W.M. Cai, *Mater. Sci. Technol.*, 12 (2004) 230.
12. L.R. Zhu, Y. Wei and Z.Q. Li, *Powder Metallurgy Industry*, 16 (2006) 26.
13. GB/T 5163-2006, Chinese Standards (GB). 2006.
14. W.H. Yang, W.T. Yang and X.Y. Lin, *Appl. Surf. Sci.*, 258 (2012) 5716.
15. F. Zhang, C. Feng, W. Li and J. Cui, *Int. J. Electrochem. Sci.*, 9 (2014) 943.
16. B. Lee, T. Lee, Y. Lee, D.J. Lee, J. Jeong, J. Yuh, H.O. Sang, H. S. Kim and S.C. Lee, *Mater. Design.*, 2014, in press.
17. M. Fusi, V. Russo, C.S. Casari, A. Li Bassi and C.E. Bottani, *Appl. Surf. Sci.*, 255 (2009) 5334.
18. H.H. Wu, B.H. Long, B.Y. Long, Y.G. Tang, H. Chang and Y.Z. Bai, *Acta Phys. Sin-ch ed*, 56 (2007) 6537.
19. Z.X. Zhang, *Titanium electrode technology (second edition)*, Metallurgical Industry Press, Beijing (2003).
20. Q. Zhang, Y. Liu, D. Zeng, J. Lin, and W. Liu, *Water. Sci. Technol.*, 64 (2011) 2023.
21. L.T. Guo, L.Z. Guo, Y.B. Zhu, C. Xu, H. Zhu and T.W. Guo, *Mater. Manuf. Process.*, 25 (2010) 696.
22. Y.W. Yao, L. Qiu, Y.H. Wang, Z. Duan and C. Wang, *Electroplating & Finishing*, 30 (2011) 54.
23. S. Sladkevich, N. Kyi, J. Gun, P. Prikhodchenko, S. Ischuk and O. Lev, *Thin Solid Films*, 520 (2011) 152.
24. X.H. Wang, T.M. Zhang, S.P. Dong and C.A. Ma, *Electrochemistry*, 16 (2010) 172.
25. G.F. Huang, Z. Xie, W.Q. Huang, S.B. Yang and L.H. Zhao, *Appl. Surf. Sci.*, 23 (2004) 13.